Stress dependence of the electronic structure of gallium

R. Griessen,* H. Krugmann, and H. R. Ott
Laboratorium für Festkörperphysik, Eidgenössische Technische Hochschule, Zürich, Switzerland
(Received 19 February 1974)

de Haas–van Alphen torque and oscillatory magnetostriction amplitudes have been measured to determine the stress dependence of several orbits of the Fermi surface of gallium. The values for $(1/A)(\partial A/\partial\sigma)$ are of the order of 20×10^{-5} bar^{-1} for uniaxial stresses along the a and b direction and typically 2×10^{-5} bar^{-1} for stresses parallel to the c axis. These data are used to identify different parts of the Fermi surface calculated by Reed. We suggest a new assignment of the orbits investigated. In addition the low-temperature thermal expansion and the uniaxial stress dependence of the superconducting transition temperature T_c have been measured to determine the stress dependence of the band-structure density of states $N(E_F)$ at the Fermi level for stresses along the main crystalline axes. The experimental $[1/N(E_F)]\,[dN(E_F)/d\sigma]$ data can be correlated to the experimental results of $(1/A)(\partial A/\partial\sigma)$ by means of a simple rigid-band model.

I. INTRODUCTION

Among the metals, gallium has always attracted a special interest because of the marked anisotropies of its physical properties. These anisotropies in the electrical and thermal conductivity,[1–6] in the thermal expansion,[1] and in the elastic constants[7,8] are not surprising, since gallium has, compared with other metals, a rather complex crystal structure. The orthorhombic crystal structure of gallium is almost base-centered tetragonal but, on the other hand, the accidental ratio of the lattice constants also leads to an almost hexagonal symmetry. Other authors have discussed the physical significance of this pseudotetragonality and pseudohexagonality.[9,10]

The complexity of the crystal lattice is also revealed in the electronic structure of gallium. Several experimental and theoretical attempts have been made to throw some light upon the complicated band structure and the Fermi surface. An almost complete list of references is given by Cracknell.[11] Although a great deal of work has been done to determine the actual Fermi surface, the most recent band-structure calculation by Reed[12] is only in qualitative agreement with de Haas–van Alphen, magnetoacoustic, radio-frequency size-effect, and magnetoresistance data.[13] The spreading of parts of the Fermi surface over several bands (up to nine in the free-electron model) is the major cause of the difficulties in interpreting quantum oscillatory effects.

One of the purposes of our investigations was to measure the stress dependence of extremal orbits in order to obtain more information for an unambiguous assignment of Fermi-surface orbits (see Sec. III). In previous publications one finds, for example, several frequency branches which are labeled as belonging to two different extremal orbits, but with the frequencies of the higher branch being twice as high as those for the lower branch. We found that such correlated branches show exactly the same behavior under uniaxial stress. This rather convincingly proves that the upper branch of such pairs is, in fact, the first harmonic of the lower branch.

As was shown in earlier work, experimental investigations of the uniaxial stress dependence of the Fermi surface provide a useful tool to test theoretical models of a metal.[14] Another purpose of this work was, therefore, to gather information on the stress dependence of several orbits which would allow a future determination of pseudopotential form factors describing the Fermi surface, as well as its changes under stress. For the determination of the stress dependence of Fermi surface orbits, we have measured the amplitude of the oscillatory magnetostriction, and of the de Haas–van Alphen torque. We shall show that g factors and information on magnetic breakdown can be obtained from the angular dependence of such amplitude measurements.

During the last few years, special attention has been paid to the so-called Lifshitz transitions caused by topology changes of the Fermi surface.[15] Near such a transition, the electronic properties of a metal are closely related to the behavior of the smallest extremal orbits of the Fermi surface. Singularities in the electronic properties of alloys have been ascribed to Lifshitz transitions induced by changes of the electron concentration or (and) by lattice distortions due to alloying.[16–20] However, only a few experimental investigations have directly and unequivocably shown the effect of a topology change of the Fermi surface.[21–23]

Apart from such singularities in the electronic properties of metals and alloys, it also seems of particular interest to study possible correlations between the ordinary stress dependence of the Fermi surface with other measurable quantities which are governed by the behavior of the electronic structure of a metal. The aim of this paper is to

show that in gallium, there is a correlation between the experimentally determined stress dependence of the electronic density of states at the Fermi level, and the stress dependence of the extremal orbits of relatively small parts of the Fermi surface. To determine the stress dependence of the band-structure density of states, we have measured the low-temperature linear thermal expansion (see Sec. IV) and the uniaxial stress dependence of the superconducting transition temperature T_c (see Sec. V). In Sec. VI we discuss a simple model, which was used to correlate the results of our experiments.

A similar investigation was made by Collins,[24] who compared values of the stress dependence of the electronic specific heat in noble metals obtained from the stress dependence of the Fermi surface, and from thermal expansion measurements, respectively.

II. SAMPLES

The samples were all single crystals grown from high-purity (5*N*) gallium[25] using a method developed by Yaqub and Cochran.[4] The crystals had the form of circular cylinders with a uniform diameter of 5 mm and lengths between 30 and 55 mm. The orientation was checked by the Laue diffraction method, and all crystals showed less than 2° deviation from the principal axes, except for the sample with the *c* axis parallel to the cylinder axis in the thermal expansion experiments. The misorientation of 3.5° leads to a somewhat larger error in that case. For the labelling of the symmetry axes we use the notation of Yaqub and Cochran.[4]

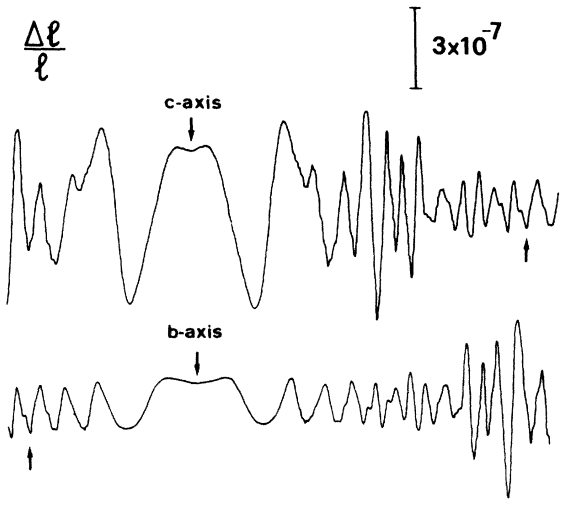

FIG. 1. Rotation diagram of a gallium single crystal for a magnetic field of 13 kOe in the bc plane. The transverse oscillatory strains are measured parallel to the *a* axis. The lower part of the diagram is the continuation of the upper curve.

The orientation of the crystals in the tail of the cryostat was also checked by means of the rotation method described by Shoenberg and Stiles.[26] The symmetry of de Haas–van Alphen or oscillatory magnetostriction rotation diagrams is very sensitive to misorientation, and to the presence of crystallites with orientations different from that of the main crystal. A typical rotation diagram obtained by slowly turning the magnetic field (4°/min) is shown in Fig. 1 for a gallium crystal with the *a* axis parallel to the cylinder axis. The length changes were measured perpendicular to the magnetic field direction, i.e., parallel to the *a* axis. In contrast to torque rotation diagrams, the oscillatory magnetostriction curve shows axes of reflection (instead of inversion points) for each symmetry plane. The larger main peak corresponds to the *b* axis, while the smaller one indicates the position of the *c* axis.

The Dingle temperatures (which are a measure of the electronic relaxation time) of the crystals used in this work were found to be typically 0.6 K.

III. OSCILLATORY MAGNETOSTRICTION AND THE STRESS DEPENDENCE OF THE FERMI SURFACE

The first oscillatory magnetostriction measurements on gallium were reported by Penz and Kushida.[27] They measured both the transverse and the parallel magnetostriction for all three axes *a*, *b*, and *c*. However, they did not determine the stress dependence of orbits, since they were mostly interested in the strain anisotropy.

As shown in previous work,[28–30] the stress dependence of Fermi-surface orbits may be calculated from the corresponding oscillatory components of the observed strains and torques by

$$\frac{1}{A}\frac{dA}{d\sigma_i} = -\frac{(\Delta l_i/l_i)}{\tau_j}\,\frac{1}{A}\left(\frac{dA}{d\Phi_j}\right)_{\Phi_0}\,, \tag{1}$$

where $\Delta l_i/l_i$ and σ_i are the uniaxial strain and stress components in the i direction, τ_j is the torque per unit volume measured in the j direction, and A is one of the extremal areas in a plane perpendicular to the field direction Φ_j. The angle Φ_j is measured in a plane perpendicular to the j direction. This relation has been discussed in detail by Griessen and Sorbello.[29,30]

In order to determine the uniaxial stress dependence of orbits of the Fermi surface, we measured the torque per unit volume and the oscillatory magnetostriction amplitudes on three gallium single crystals. The samples were 32 mm long, and for each sample, one of the axes *a*, *b*, or *c* was chosen to be parallel to the cylinder axis. The measurements were done at 1.3 K in magnetic fields up to 22 kOe provided by a conventional

electromagnet with a homogeneity better than 5×10^{-5} over the sample volume. Both the strain and torque amplitudes were measured in a direction perpendicular to the field (for example, along the c axis as a function of the magnetic field orientation in the ab plane for a sample with the c axis parallel to the cylinder axis).

The oscillatory length changes and the torque were measured with a "dilatorquemeter." A "dilatorquemeter" is a device which allows the *simultaneous* measurement of the torque and length changes on the *same* specimen. The sensitivity of the dilatometer part ($\Delta l/l < 10^{-10}$) and of the torque-meter part (0.1 dyn cm^{-2} for the torque per unit volume, with a compliance of 2×10^{-7} rad dyn^{-1} cm^{-1}) of the dilatorquemeter is comparable to that of the devices described in Refs. 31 and 32. The great advantage of a dilatorquemeter is that not only can the amplitudes of the torque and length changes be measured at the same time, but that the relative phases of both signals may be reliably determined. The *sign* of the uniaxial stress dependence of orbits is therefore easily found by means of a phase analysis of the signals. If both signals are in phase, then the stress dependence of the orbit under investigation will be positive (or negative) depending on the sign of the angular variation of A (negative or positive). The amplitude, frequency, and phase of the recorded oscillations are easily determined by Fourier analysis.

The oscillation frequencies are shown in Fig. 2 as a function of the magnetic field orientation in the ab, bc, and ac planes. All observed frequencies, including the harmonics, are shown in the figure. The frequencies determined both from torque and from oscillatory magnetostriction measurements are in good agreement with the data of Goldstein and Foner,[33] Condon,[34] and Goy *et al.*[35] From a comparison of Figs. 1 and 2 of Goldstein and Foner's paper with our results, it seems that their VIII and IX branches and the unlabelled branch which crosses branch IV are in fact first harmonics of their branches I (here γ_c) II (here γ_a), and III A, B (here ϵ_b, ξ_b). The λ branch has also been observed by Goldstein and Foner in the ab plane, but the ω and κ branches are new. In a small angular range around 70° from the b axis in the bc plane, we observed a frequency halfway between the ϵ_a and ξ_a branches which seems to be generated by magnetic breakdown between ϵ_a and ξ_a. Neither in the torque nor in the oscillatory magnetostriction were we able to detect oscillations from the extremely-low-frequency branch δ observed by Condon.[34] This is very surprising, since from general considerations we would expect such a small pocket to be extremely sensitive to lattice distortions. On the other hand, it should be pointed out that the existence of such low-frequency oscillations is extremely difficult to prove, because only about one period is observable between 2 and 30 kOe. The angular dependence of the oscillatory magnetostriction and torque per unit volume amplitudes is shown in Figs. 3, 4, and 5 for the three symmetry planes ab, bc, and ac.

For orbits not affected by magnetic breakdown

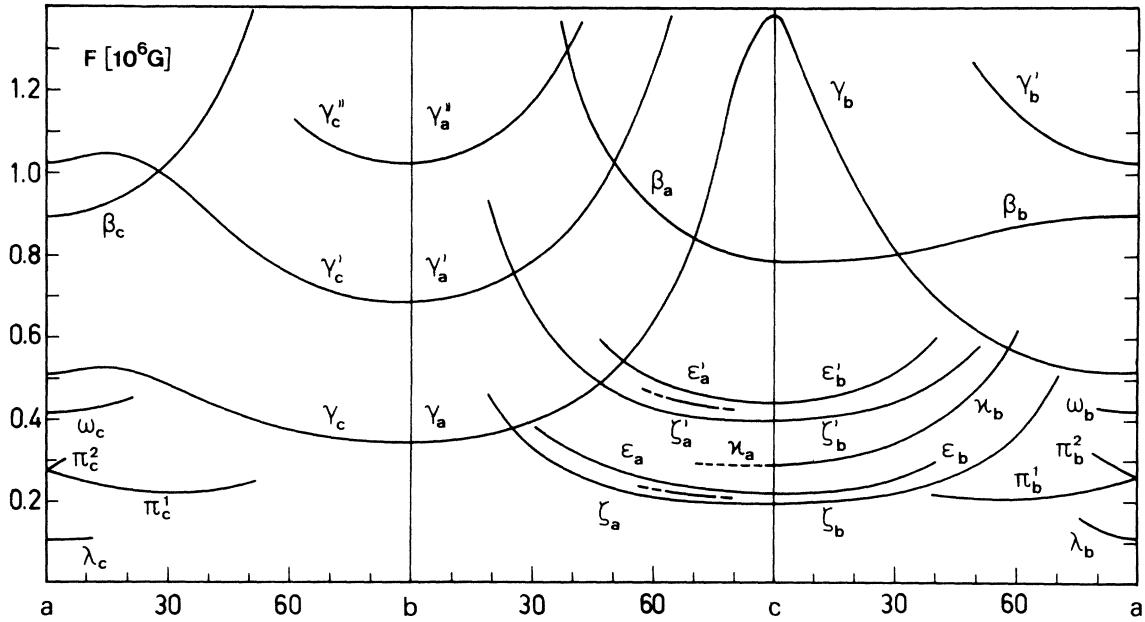

FIG. 2. Experimental oscillation frequencies vs magnetic field orientation obtained from oscillatory magnetostriction and de Haas–van Alphen torque measurements. The harmonic branches are also displayed and indicated by apostrophes.

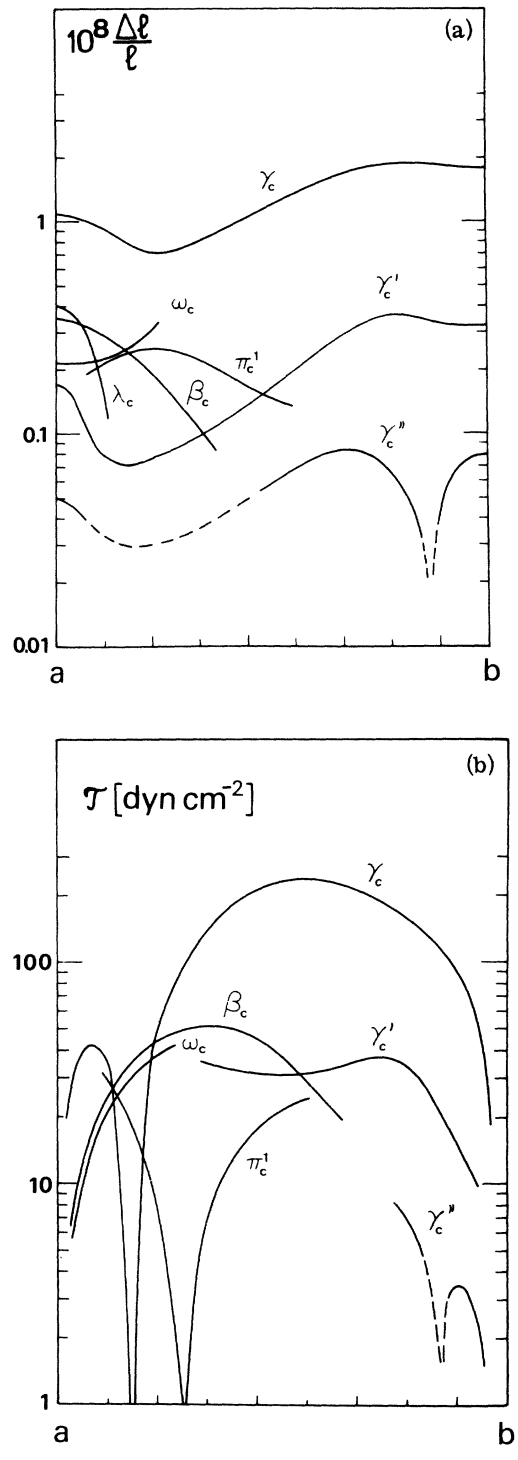

FIG. 3. (a) Angular variation of the transverse oscillatory magnetostriction amplitude for magnetic field directions in the *ab* plane. The relative errors are of the order of 5%. The amplitudes are given for a field $H = 15$ kOe, (b) Angular variation of the torque per unit volume amplitude for magnetic field directions in the *ab* plane. The torque is measured parallel to the *c* axis. The experimental points are omitted for clarity.

with a spin-splitting amplitude factor $\cos[(gm^*/m) \times (\pi/2)]$ significantly different from zero, we expect that, for temperatures and fields with $T/H > 10^{-5}\, m/m^*$,

$$\ln\frac{\Delta l/l}{F} = r\alpha\beta F\left(\frac{T+T_D}{H}\right) + \text{const} \quad , \tag{2}$$

where

$$\alpha = 2\pi^2 k_B m/e\hbar = 1.47\times 10^5 \text{ G/K} \tag{3}$$

and r is the harmonic number ($r = 1$ for the fundamental frequency), T_D is the Dingle temperature and F the fundamental frequency of the oscillation of the orbit under investigation. Relation (2) is derived from the Lifshitz-Kosevich[36] theory of the de Haas–van Alphen effect, and is true if (i) the frequency F is proportional to the effective mass, i.e., $m^*/m = \beta F$, (ii) the curvature factor $|\partial^2 A/\partial k^2|$ and the Dingle temperature are slowly varying functions of the orientation, and (iii) the uniaxial stress dependence $(1/A)(dA/d\sigma)$ does not depend on the orientation. Assumptions (i) and (iii) have been discussed in detail by Shepherd and Gordon[37] and also by Griessen and Sorbello.[29,30] The constancy of the stress dependence is also clearly demonstrated in Fig. 5 for almost all orbits. Relation (2) is rather nicely satisfied for the β (except β_b), κ, π, and γ (except γ_c'') branches. This behavior has also been found for most of the orbits investigated in simple metals.[29,30]

We now proceed to discuss the amplitude data for each orbit.

A. β orbit

The β orbits correspond to cross sections of a closed pocket of the Fermi surface which has been identified by Reed[12] as the seventh-band-electron "saucer" on the T-symmetry line of the Brillouin zone. In the *ac* plane, the amplitude of $\Delta l/l$ and τ vanishes for a field direction approximately 52° from the *c* axis. This means that[36] $\cos[(gm^*/m) \times (\frac{1}{2}\pi)] = 0$, and with $m^*/m = 0.2$ from Condon's data,[34] we find a g factor $g = 5 + n\times 10$. The vanishing of the oscillation amplitude is also suggested by the magnetothermal oscillation data of Goy *et al.*,[35] and it explains why Goy *et al.* were able to observe the much weaker oscillations (labelled σ in Ref. 35) with frequencies around 1.6 MG. It seems to us that this σ branch is in fact the first harmonic γ_b' in Fig. 1. The sharp decrease of the strain amplitude near *c* in the *ac* plane is certainly due to magnetic breakdown between the seventh-band saucer and the sixth-band hole monster. In the *bc* plane, magnetic breakdown affects the strain amplitude for all orientations (not only near the *c* axis), and sharp changes in the amplitude do not exist. This is in good qualitative agreement with Reed's Fermi surface.

B. γ orbits

The γ orbits have been attributed to the sixth-band hole pancake situated on the T line of the Brillouin zone. For most of the orientations, we observed a strong harmonic content, in agreement with the low values for the effective masses found by Condon.[34] For the second harmonic γ_c'', the oscillation amplitudes vanish for a magnetic field orientation near the b axis. Assuming $m^*/m = 0.055$,[33] we find $g = 6.06 + n \times 12.12$. For $n = 3$ we obtain $g = 42.4$, and this is in good agreement with the value of $43.4 + n \times 72.7$ obtained from an amplitude and phase analysis of the γ, γ', and γ'' oscillations. Shapira and Lax[38] calculated the g factors using an effective mass $m^*/m = 0.069$. Their results are $g = 0.94 \pm 0.08$, 30 ± 2, and 32 ± 2. The latter two values would be 37.6 ± 2.5 and 40.1 ± 2.5 using $m^*/m = 0.055$.

With the same analysis of the harmonics, we found that the product gm^* remains constant within a few percent if the orientation is changed. A very weak anisotropy was predicted theoretically by Pippard,[39] and was also found by Bennett and Falicov[40] and Myers and Bosnell[41] in zinc.

C. ϵ, ζ orbits

These orbits have frequencies which are only about 10% different from one another and show a minimum for the field along the c axis. Condon found for these two orbits $m^*/m = 0.08$, and it is therefore not surprising that first harmonic oscillations could be detected. Strain amplitudes show a marked minimum for field orientations about 15° from the c axis. Around this orientation, we observed a third branch with frequencies equal to $\frac{1}{2}F_\epsilon + \frac{1}{2}F_\zeta$. These two experimental facts strongly suggest that this extra frequency is generated by magnetic breakdown between two concentric orbits which are nearly degenerate at two diametrically opposed points. Such a situation would occur for orbits across the pseudohexagonal face of the Brillouin zone, where the degeneracy is only lifted by introduction of spin-orbit coupling. In Reed's model, the ϵ and ζ branches would therefore correspond to the fifth- and sixth-band hole ellipsoids at point K of the Brillouin zone. These ellipsoids are degenerate along XRL, since spin-orbit coupling does not lift the degeneracy along this symmetry line.[42] Any assignment of orbits near point X is, however, very uncertain, because of the great complexity of the band structure at this point.

D. κ, λ, and ω orbits

The frequency branches κ and ω have not been observed previously. The angular dependence of κ_b and the magnitude of the frequency suggest that the κ orbits correspond to sixth-band hole-monster

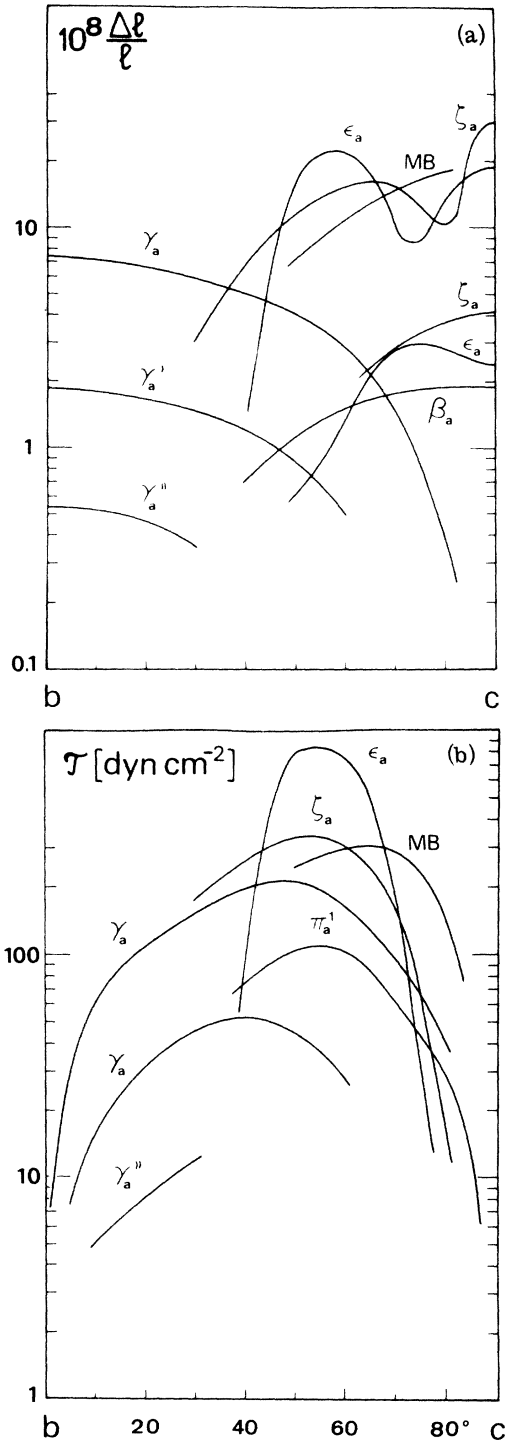

FIG. 4. (a) Angular variation of the transverse oscillatory magnetostriction amplitude for magnetic field directions in the bc plane. The oscillatory strain amplitude for orbits due to magnetic breakdown between ϵ_a and ζ_e orbits is indicated by MB. (b) Angular variation of the torque per unit volume amplitude for magnetic field directions in the bc plane. The torque is measured parallel to the a axis. The experimental points are omitted for clarity.

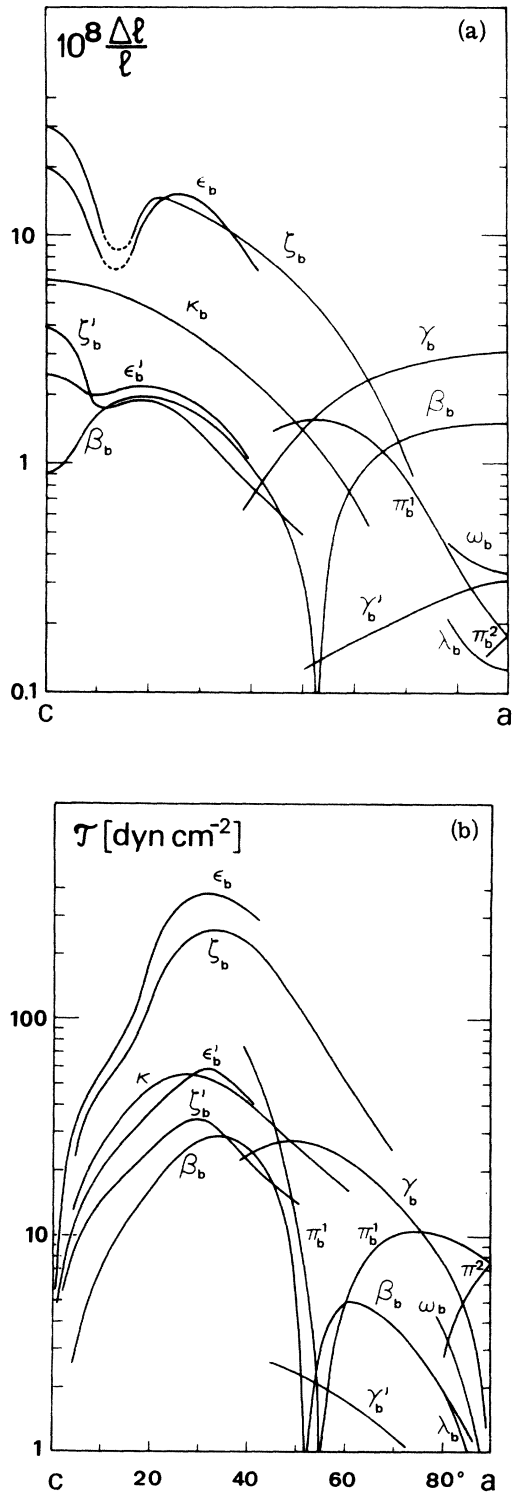

FIG. 5. (a) Angular variation of the transverse oscillatory magnetostriction amplitude for magnetic field directions in the *ca* plane. (b) Angular variations of the torque per unit volume amplitude for magnetic field directions in the *ca* plane. The torque is measured parallel to the *b* axis. The experimental points are omitted for clarity.

cross sections labelled *g* by Reed (see Fig. 4 of Ref. 12). The ω orbits were observed over a small angular range around the *a* axis. Considering only the magnitude of the frequencies, one might be tempted to attribute this branch to *f* orbits (in Reed's notation) of the sixth-band hole monster. Since Reed mentioned that these *f* orbits are extremely sensitive to changes in the Fermi energy (an increase of E_F by about 2 mRy makes them disappear), we would therefore rather associate the *f* branch to the λ orbits, which are also very sensitive to lattice distortions. The highest value for $(1/A)(dA/d\sigma)$ was in fact found for the λ orbits (see Table I).

E. π orbits

The π orbits have been attributed to the seventh-band butterfly located at point *N* of the Brillouin zone. The π^1_c and π^2_c branches are also reported by Goy *et al.* The vanishing of the torque amplitude at $\Phi = 25°$ from *a* in the *ab* plane, and at $\Phi = 55°$ from *c* in the *ac* plane, indicates a frequency minimum.

The uniaxial stress dependence $(1/A)(dA/d\sigma_i)$ of orbits (see Fig. 6 and Table I) has been obtained from the data shown in Figs. 3–5 by means of relation (1). As in aluminum, indium, zinc, and magnesium, we found a very weak angular dependence of $(1/A)(dA/d\sigma_i)$ for all orbits. In a previous paper,[29] we have shown that this constancy may be traced to the cylindrical nature of the Fermi-surface portions where the orbits are located.

For the β and γ orbits, we found that the stress dependence deduced from the amplitude of the various harmonics gives the same result as the fundamental. This is in agreement with theoretical predictions based on the Lifshitz-Kosevich theory, and is due to the fact that $(1/A)(dA/d\sigma_i)$ appears as a multiplicative factor in the oscillatory strain amplitude.[28]

A surprising result is that, for a uniaxial stress parallel to the *c* direction, $(1/A)(dA/d\sigma_i)$ is about one order of magnitude smaller than for a stress along the *b* axis. From the pseudohexagonality of the gallium lattice ($a = 4.5151$, $b = 4.4881$, and $c = 7.6318$ Å),[9(b)] one would expect, at first sight, that the properties relative to the *b* and *c* axis are very similar. However, it follows from our stress-dependence data that small lattice distortions may have quite drastic effects on the shape of the Fermi surface. To illustrate this sensitivity of the Fermi surface, we have calculated the uniaxial tensions necessary to make the gallium lattice hexagonal. Using the low-temperature elastic constants of Lyall and Cochran,[7] we found that hexagonality could be achieved with a uniaxial tension of 14.5 kbar along the *c* axis, or with a

tension of 37.0 kbar along the a axis, or with a uniaxial compression of 8.9 kbar along the b axis. For each of these critical stresses, the γ orbits would increase in size while the ϵ and ζ orbits would completely disappear, thus changing the topology of the Fermi surface at point X. For $\sigma_a = 37.0$ kbar, the β orbits would also disappear. This clearly shows that pseudohexagonality (or tetragonality) arguments are of no physical meaning for the discussion of electronic properties.

Another noteworthy result is that, for most of the orbits, the signs for $(1/A)(dA/d\sigma_i)$ are opposite for a stress parallel to the a axis and for a stress parallel to the b axis. We shall see in Secs. IV and V that a similar anisotropy is found in other physical properties of gallium.

IV. THERMAL EXPANSION

At low temperatures, the linear thermal expansion coefficient is usually written as the sum of an electronic and a lattice contribution

$$\alpha(T) = aT + bT^3 + cT^5 + \cdots \ , \tag{4}$$

where the linear term in temperature is due to electronic excitations, and the other terms are due to lattice anharmonicities. Usually, c is very much smaller than a and b and, at temperatures below a few degrees Kelvin, we expect $\alpha(T)$ to vary with temperature according to the simpler equation

$$\alpha(T) = aT + bT^3 \ . \tag{5}$$

To relate a with other measurable quantities, we use the Grüneisen relation[43]

$$\gamma_i = \alpha_i \Omega / c_p \kappa_i \ , \tag{6}$$

where α_i is the linear thermal expansion coefficient in the i direction, Ω is the atomic volume, c_p is the specific heat at constant pressure, and

TABLE I. Experimental values for the uniaxial stress dependence of various orbits of the Fermi surface of gallium. σ_i is a uniaxial tension, given in 10^5 bar, in the i direction.

Orbit	F (10^6 G)	$\frac{1}{A}\frac{dA}{d\sigma_a}$	$\frac{1}{A}\frac{dA}{d\sigma_b}$	$\frac{1}{A}\frac{dA}{d\sigma_c}$
β[100]	0.895	···	6.4 ± 0.5	−0.6 ± 0.1
β[001]	0.795	−10 ± 1	6.6 ± 0.5	···
γ[100]	0.515	···	−40 ± 3	2.3 ± 0.3
γ'[100]	1.030	···	−43 ± 6	···
γ[010]	0.345	20 ± 1	···	2.3 ± 0.3
γ'[010]	0.690	20 ± 2	···	2.4 ± 0.5
γ''[010]	1.035	20 ± 3	···	···
ϵ[001]	0.225	−16 ± 1.5	22 ± 2	···
ϵ'[001]	0.45	···	24 ± 3	···
ζ[001]	0.20	−20 ± 3	25 ± 2	···
ζ'[001]	0.40	···	24 ± 3	···
κ[001]	0.29	···	−50 ± 6	···
π^1[100]	0.27	···	−17 ± 5	−2.5 ± 0.4
λ[100]	0.105	···	−230 ± 100	···
ω[100]	0.42	···	−2.3 ± 2	−2.3 ± 0.3

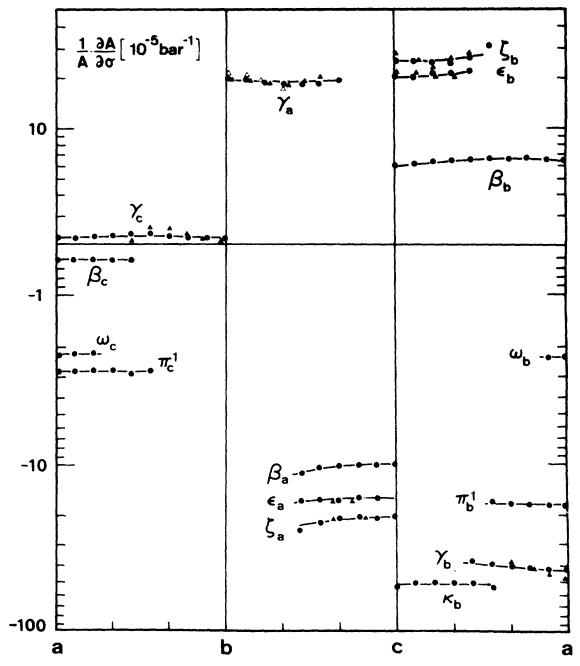

FIG. 6. Angular variation of the uniaxial stress dependence of gallium Fermi-surface orbits. σ is a uniaxial tension perpendicular to the plane in which the magnetic field direction is varied. Dots, stress dependence obtained from analysis of fundamental frequencies; closed triangles, stress dependence obtained from analysis of first harmonics; open triangles, stress dependence obtained from analysis of second harmonics.

κ_i is the adiabatic uniaxial compressibility. At sufficiently low temperatures, it is possible to separate the electronic parts of the thermal expansion coefficient and the specific heat, and to determine the electronic Grüneisen parameter γ^e

$$\gamma_i^e \equiv \left(\frac{\partial \ln \Gamma}{\partial \ln l_i}\right)_{\sigma_j} = \frac{a_i \Omega}{\Gamma \kappa_i} \ , \tag{7}$$

where Γ is the electronic-specific-heat parameter. This formula is valid for a uniaxial stress applied to a crystal with free sides.

The electronic specific heat is related to the density of states through the formula[44]

$$\Gamma = \tfrac{1}{3}\pi^2 k_B^2 N(E_F)(1+\lambda) \ , \tag{8}$$

where k_B is Boltzmann's constant, λ is the electron-phonon interaction parameter, and $N(E_F)$ is the band-structure density of states. It is thus clear from formulas (4), (7), and (8) that measurements of the linear thermal expansion can give information on the stress or volume dependence of the density of states, if, at the same time, the volume dependence of λ is known. This question will be investigated in Sec. V.

To our knowledge, no data exist for the thermal

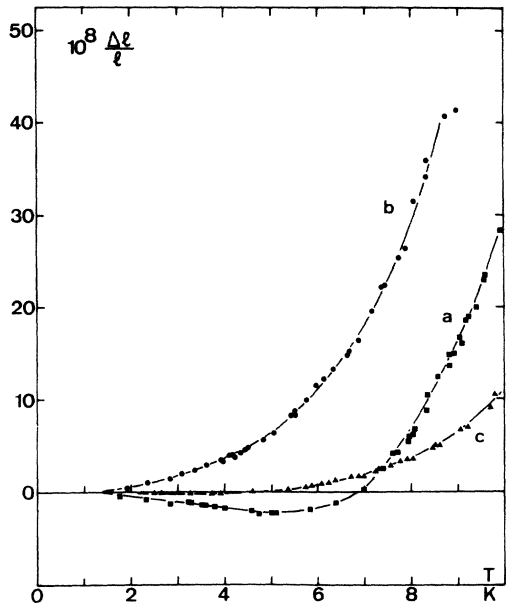

FIG. 7. Relative length changes due to thermal expansion of gallium single crystals along the principal symmetry axes, between 1.4 and 10 K.

expansion of gallium below liquid-nitrogen temperatures. Between 78 K and room temperature, the only reliable measurements are due to Powell,[1] who found strong anisotropies for α_i. We have therefore measured the thermal expansion of gallium single crystals along the a, b, and c axis between 1.4 and 10 K. The samples were 55 mm long, and they were mounted in a capacity cell which allowed the crystals to be thermally isolated from the sample holder. Both the sample and the sample holder were initially cooled to 1.4 K, and the specimens were then heated to appropriate temperatures up to 10 K, while the capacity cell was thermally anchored to the surrounding He^4 bath. For the largest heating powers, the sample holder was not heated above 2 K, thus giving a negligible error in the length change measurements. The sensitivity for relative length changes achieved in these experiments was of the order of 5×10^{-10}. The temperatures were measured with calibrated carbon resistors on both the sample and the sample holder. We estimate the error in the temperature measurements to be ± 0.002 K at the lowest, and $\pm$ 0.02 K at the highest temperatures.

The results of the experiments are shown in Fig. 7, where we have plotted the relative length changes against temperature. From these data, the numerical values of a and b in Eq. (5) can be determined by plotting $[\Delta l(T)/l(T)]/T^2$ against T^2. In that case, $\Delta l(T)$ is the total expansion from 0 K to the appropriate temperature T. The total length change from 0 to 1.4 K has been determined by extrapolation, considering that $\alpha(T=0)=0$. It may be seen that below 5 K ($T<\Theta_D/60$), this plot yields a straight line, thus confirming the validity of Eq. (5) in this temperature region. Above 5 K, the influence of the T^5 term is obvious. The solid lines in Fig. 8 are least-square fits to the experimental points; we obtain the following values for the linear thermal expansion coefficients along the a, b, and c axis:

$$\alpha_a = (-34\pm2)\times10^{-10}T + (12.8\pm2)\times10^{-11}T^3 + (9.8\pm1)\times10^{-13}T^5 ,$$

$$\alpha_b = (+32\pm2)\times10^{-10}T + (13.2\pm2)\times10^{-11}T^3 + (11.7\pm1)\times10^{-13}T^5 ,$$

$$\alpha_c = (-7.5\pm1)\times10^{-10}T + (6.2\pm1)\times10^{-11}T^3 - (0.8\pm0.1)\times10^{-13}T^5 ,$$

and

$$\alpha_\Omega = -(9.5\pm1)\times10^{-10}T + (32.2\pm2)\times10^{-11}T^3 + (20.7\pm2)\times10^{-13}T^5 ,$$

where α_Ω is the volume thermal expansion coefficient.

Here we are mainly interested in the electronic part of the thermal expansion. The lattice thermal expansion will be discussed elsewhere,[45] together with data at higher temperatures.

Using specific-heat data of Philips[46] and of Seiden and Keesom,[47] we have calculated the electronic Grüneisen parameter for uniaxial stress and for hydrostatic pressure. The results are shown

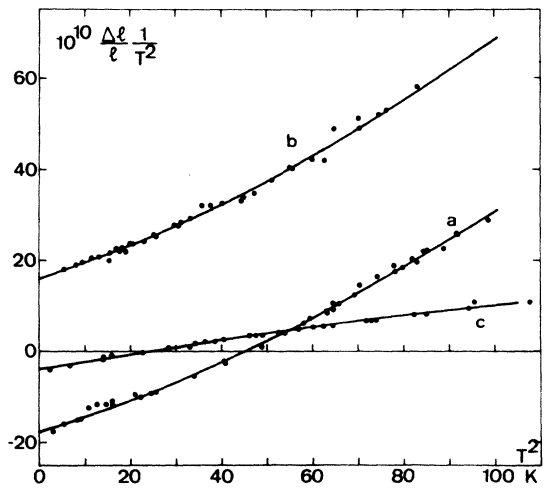

FIG. 8. Plot of $\Delta l(T)/l(T)T^2$ vs T^2 for the a, b, and c axes of gallium single crystals. The solid lines are least-square fits to the experimental points.

TABLE II. Stress and volume dependence of various parameters obtained from measurements of the thermal expansion and of the stress dependence of the superconducting transition temperature T_c.

	a	b	c	Hydrostatic
$\frac{\partial \ln\Gamma}{\partial \ln l_i}$	-14.0 ± 1	$+10.0 \pm 1$	-3.1 ± 0.8	-1.1 ± 1
$\frac{10^5 \partial T_c}{\partial \sigma_i}$ (K bar^{-1})	-0.5 ± 0.1	$+1.5 \pm 0.1$	$+0.45 \pm 0.1$	$+1.45 \pm 0.3$
$10^{13}\ \frac{\partial \ln\Omega}{\partial \sigma_i}\left(\frac{\text{cm}^2}{\text{dyn}}\right)$	5.1	6.7	4.7	16.6
γ_i^G	0.9	1.85	1.55	1.5
$\frac{\partial \ln\lambda}{\partial \ln l_i}$	-1.4 ± 0.2	$+3.5 \pm 0.4$	$+1.75 \pm 0.2$	$+1.75 \pm 0.2$
$\frac{\partial \ln N(E_F)}{\partial \ln l_i}$	-13.6 ± 1.1	$+9.0 \pm 1.1$	-3.6 ± 0.9	-1.6 ± 1

in Table II. The data for the compressibilities were taken from work of Lyall and Cochran.[7]

The most obvious features are that the stress dependence of the electronic specific heat is of opposite sign for stresses along the a and b axes, and significantly smaller for stresses parallel to the c axis. As for the stress dependence of Fermi-surface orbits, no arguments based on the pseudosymmetries of the crystal lattice can be used to discuss this strong anisotropy.

V. STRESS DEPENDENCE OF THE SUPERCONDUCTING TRANSITION TEMPERATURE

As we have mentioned in Sec. IV, the stress dependence of the electronic specific heat includes a term which arises from the stress dependence of the electron-phonon coupling parameter λ:

$$\frac{\partial \ln\Gamma}{\partial \sigma_i} = \frac{\partial \ln N(E_F)}{\partial \sigma_i} + \frac{\lambda}{1+\lambda}\frac{\partial \ln\lambda}{\partial \sigma_i} \quad . \tag{9}$$

A simple way of determining values of $\partial \ln\lambda/\partial\sigma_i$ is based on the analytic expression of the superconducting transition temperature due to McMillan[48]

$$T_c = (\Theta_D/1.45)e^{-1/g} \ , \tag{10}$$

where Θ_D is the Debye frequency of the lattice and where g depends on λ and μ^*, the Coulomb pseudopotential of Morel and Anderson.[49] According to McMillan we have

$$g = \frac{\lambda - \mu^* - 0.62\lambda\mu^*}{1.04(1+\lambda)} \quad . \tag{11}$$

As in earlier work on this subject,[50] we neglect the stress dependence of μ^* and we obtain

$$\frac{\partial \ln g}{\partial \sigma_i} = \frac{1+0.38\mu^*}{\lambda - \mu^* - 0.62\lambda\mu^*}\frac{\lambda}{1+\lambda}\frac{\partial \ln\lambda}{\partial \sigma_i} \quad . \tag{12}$$

On the other hand we can calculate $(\partial \ln g/\partial \ln l_i) = (1/\kappa_i)(\partial \ln g/\partial\sigma_i)$ using formula (10):

$$\frac{\partial \ln g}{\partial \ln l_i} = \frac{(\partial \ln T_c/\partial \ln l_i)^{\text{expt}} + \gamma_i^G}{\ln(\Theta_D/1.45T_c)} \ , \tag{13}$$

where γ^G is the lattice Grüneisen parameter

$$\gamma_i^G = -\left(\frac{\partial \ln\Theta_D}{\partial \ln l_i}\right)_{\sigma_j} \quad . \tag{14}$$

Combining Eqs. (12) and (13), we can finally write

$$\frac{\lambda}{1+\lambda}\frac{\partial \ln\lambda}{\partial \ln l_i} = \frac{\lambda - \mu^* - 0.62\lambda\mu^*}{1+0.38\mu^*} \times \frac{(\partial \ln T_c/\partial \ln l_i)^{\text{expt}} + \gamma_i^G}{\ln(\Theta_D/1.45T_c)} \quad . \tag{15}$$

Our experimental values of $\partial \ln T_c/\partial \ln l_i$ originate from measurements of the length change of gallium single crystals at the magnetic-field-induced transition from the superconducting to the

TABLE III. Quantities used in the calculation of $[1/N(E_F)][\partial N(E_F)/\partial\sigma_i]$ from $(1/A)(\partial A/\partial\sigma_i)$ experimental data in a rigid-band-model approximation.

Orbit	F (10^8 G)	σ_i	$(\mu_\perp^{(1)}\mu_\perp^{(2)})^{1/2}$ [a]	$(\mu_\perp^{(1)}\mu_\perp^{(2)}A)^{1/2}\frac{1}{A}\frac{dA}{d\sigma}$ (cm^{-1} bar^{-1})
γ[100]	0.515	σ_b	0.14	−391
γ[100]	0.515	σ_c	0.14	22.4
γ[010]	0.345	σ_a	0.19	219
β[100]	0.895	σ_b	0.37	221
β[100]	0.895	σ_c	0.37	−21.1
β[001]	0.795	σ_a	0.37	−326
ξ[001]	0.20	σ_a	0.32	−280
ξ[001]	0.20	σ_b	0.32	349
ϵ[001]	0.225	σ_a	0.32	−237
ϵ[001]	0.225	σ_b	0.32	327

[a] Estimated from Condon's value given in Ref. 12 and assuming m^*/F = const for each frequency branch (see Sec. III). For a magnetic field parallel to the z direction, $\mu_\perp^{(1)}$ and $\mu_\perp^{(2)}$ correspond to μ_x and μ_y.

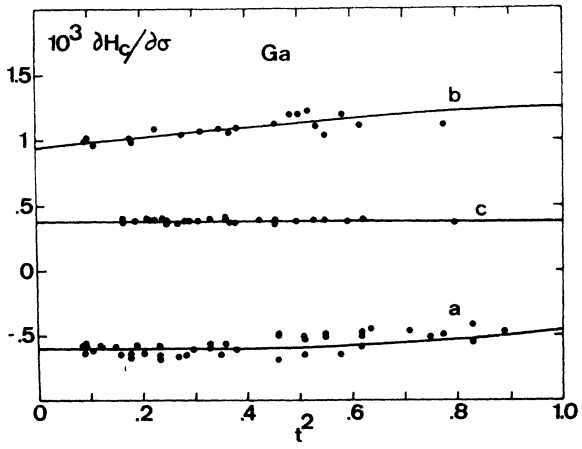

FIG. 9. Temperature dependence of $\partial H_c/\partial\sigma_i$ for stresses along the a, b, c axes of gallium single crystals; $t = T/T_c$.

normal state. A short description of these experiments has been given in an earlier publication.[51] Direct measurements of the stress dependence of T_c by directly applying a uniaxial stress to the crystal are less suitable, since we actually need the values of $\partial T_c/\partial\sigma_i$ at zero pressure, and length change measurements are carried out under experimental conditions that correspond to those of the investigations on the oscillatory magnetostriction and the thermal expansion. From the length change measurements we obtain the stress dependence of the critical field H_c according to the formula

$$\frac{l_{ni}-l_{si}}{l_{si}} = -\frac{1}{4\pi}H_c\left(\frac{\partial H_c}{\partial\sigma_i}\right)_{T,\sigma_j} - \frac{H_c^2}{8\pi}\frac{1}{V}\left(\frac{\partial V}{\partial\sigma_i}\right)_{T,\sigma_j} . \tag{16}$$

In the case of gallium, the second term on the right-hand side can be neglected. The temperature dependence of the critical field is usually written in the form

$$H_c = H_0 f(t) \quad , \tag{17}$$

where $t = T/T_c$.

Differentiation with respect to stress leads to

$$\frac{\partial H_c}{\partial\sigma_i} = \frac{H_0}{\partial\sigma_i} f(t) - H_0 t f'(t)\frac{1}{T_c}\frac{\partial T_c}{\partial\sigma_i} \quad , \tag{18}$$

where $f' = \partial f/\partial t$.

From the temperature dependence of $\partial H_c/\partial\sigma_i$, which is shown in Fig. 9, it is possible to deduce values for the stress dependences of T_c. Our results are given in Table II, together with the values of $\partial\ln\lambda/\partial\ln l_i$ obtained from Eq. (15). The lattice Grüneisen parameter has been taken from high-temperature thermal expansion measurements.[45] This choice for γ^G has recently been discussed by Ott and Sorbello.[50] In Fig. 9, it is interesting to note that also the stress dependences of the critical field H_c show an anisotropy similar to those mentioned in Secs. III and IV.

At this point we should remember that $\partial\ln\Gamma/\partial\sigma_i$ can also be deduced from the well-known Rutgers formula in the form

$$\Gamma = (1/4\pi)(H_0^2/T_c^2) f''(0) \quad . \tag{19}$$

This procedure, however, requires a subtraction of two almost equally large numbers, and the relative error is therefore very large. In addition, note that the application of Eq. (19) for a determination of $\partial\ln\Gamma/\partial\sigma$ implicitly assumes the validity of the similarity principle, which is not ascertained in the case of gallium. (Any violation of the similarity principle strongly affects the value of $\partial\ln\Gamma/\partial\sigma$, but is much less effective on the determination of $\partial T_c/\partial\sigma$.) We thus give little weight to the values so obtained, and omit any numerical data.

VI. DISCUSSION

We are now in a position to calculate the stress and volume dependence of the density of states using Eq. (9). The results are shown in Tables II–IV for stresses of volume changes along the a, b, and c axis, as well as for hydrostatic pressure. The most obvious result, apart from the observed anisotropies, is that band-structure effects are one order of magnitude larger than contributions due to the stress dependence of the electron-phonon interaction. A similar situation has also been described by Schirber and Van Dyke for $AuGa_2$.[23] In gallium, $\partial\ln\lambda/\partial\sigma_i$ is of the same order of magnitude as in the simple metals aluminum, lead, or indium. In these metals, however, band-structure effects are far less effective, and the stress dependence of the electronic specific heat is strongly influenced by $\partial\ln\lambda/\partial\sigma_i$.[50]

TABLE IV. Comparison of values of $[1/N(E_F)]$ $[\partial N(E_F)/\partial\sigma_i]$ obtained by different methods.

Method of determination	$\frac{1}{N}\frac{dN}{d\sigma_a}$	$\frac{1}{N}\frac{dN}{d\sigma_b}$ (10^{-5} bar^{-1})	$\frac{1}{N}\frac{dN}{d\sigma_c}$
Thermal expansion $+dT_c/d\sigma$ data	−0.69	+0.60	−0.17
Oscillatory magnetostriction Eq. (21), $\nu_\epsilon = \nu_\zeta = 1$	−0.27	+0.18	<0
Oscillatory magnetostriction Eq. (21), $\nu_\epsilon = \nu_\zeta = 2$	−0.48	+0.47	<0

Remembering the explicit expression of McMillan for λ

$$\lambda = N(E_F)\langle J^2\rangle / M\langle\omega^2\rangle \ , \tag{20}$$

where $\langle J^2\rangle$ is an average of the electron-phonon matrix element over the Fermi surface, M is the atomic mass, and $\langle\omega^2\rangle$ is an average of the square of the phonon frequency, our result would then suggest that $\langle J^2\rangle$ has a stress dependence of the same order of magnitude as that of $N(E_F)$, but of opposite sign, thus leading to $\langle J^2\rangle \propto 1/N(E_F)$.

Another interesting feature is the negative pressure derivative of $N(E_F)$ for hydrostatic pressure leading to a negative volume expansion coefficient in the temperature region where electronic effects are dominant. The same result has also been obtained by Palmy, who studied the influence of hydrostatic pressure on the superconducting parameters in gallium.[52]

The stress dependence of the density of states determined from thermal expansion data and $dT_c/d\sigma$ data shows an anisotropy similar to that of the stress dependence of most of the extremal areas of the Fermi surface. This suggests that a rather simple correlation must exist between $[1/N(E_F)][dN(E_F)/d\sigma]$ and the various $(1/A)(dA/d\sigma)$. Without analytic models for the band structure it is, however, impossible to correlate directly the stress dependence of the density of states and the stress dependence of the de Haas–van Alphen orbits. For simple metals one would determine, in the framework of a pseudopotential calculation, a form factor describing the Fermi surface as well as its stress dependence, and then calculate the stress dependence of the density of states. Such a procedure cannot be applied to gallium, because the Fermi surface is only qualitatively described by the existing band-structure calculations.[12]

In the theory of electron transitions, Lifshitz showed that the pressure dependence of electronic properties of metals may be dominated by the contribution of the smallest pockets of the Fermi surface, although their contribution to the total density of states is small. An illustration of the importance of small pockets is found in zinc, where the size of the extremely small third-band needles strongly affects the steady susceptibility and its stress dependence.[53] In a parabolic band model, the contribution to the total density of states at the Fermi energy is proportional to $(\mu_x\mu_y A_z)^{1/2}$ if μ_x and μ_y are the cyclotron effective masses in the directions x and y perpendicular to the field direction z. A_z is the corresponding extremal orbit. For the stress dependence of the density of states we therefore have in a rigid-band model,

$$\frac{1}{N(E_F)}\frac{dN(E_F)}{d\sigma} = \frac{2}{3}\frac{1}{\Omega}\frac{d\Omega}{d\sigma} + \frac{1}{N(E_F)}\frac{\Omega}{2\pi^{5/2}}\frac{m}{\hbar^2} \times \sum_i \nu_i (A_{iz}\mu_{ix}\mu_{iy})^{1/2}\frac{1}{A_{iz}}\frac{dA_{iz}}{d\sigma} \tag{21}$$

where ν_i gives the number of identical Fermi-surface pieces, and the summation is over different extremal orbits of the Fermi surface. Among these orbits, the most effective are small extremal orbits which belong to nearly cylindrical pieces of the Fermi surface. Large de Haas–van Alphen oscillations are generally associated with small values for $|\partial^2 A/\partial k_\parallel^2| \approx \mu_\parallel/\mu_\perp$ and large oscillatory strains with large $(1/A)(dA/d\sigma)$. Thus, the extremal orbits which play an important role in the stress dependence of the density of states are those which can easily be detected in low-field de Haas–van Alphen and oscillatory magnetostriction experiments. For the evaluation of the sum in relation (21), we used the values quoted in Table I. In agreement with the orbits assignment discussed in Sec. III, $\nu_i = 2$ for all orbits, except for the ϵ and ζ branches where $\nu = 1$, if these branches are associated with the fifth- and sixth-band hole ellipsoids at point X. The stress dependence of the density of states evaluated by means of Eq. (21) is smaller by a factor 3, than the corresponding value determined from thermal expansion and $dT_c/d\sigma$ data. The quantitative agreement could be greatly improved if the ϵ and ζ branches belonged to Fermi-surface pockets on the $XSS'L$ or XRL line, rather than to hole ellipsoids at X. Then $\nu_i = 2$ for all orbits, and the corresponding $[1/N(E_F)] \times [dN(E_F)/d\sigma]$ given in Table IV are found to be in surprisingly good agreement with the experimental values. For both choices of ν_i, the anisotropy of the stress dependence of the density of states is in agreement with the experimental values.

Relation (21) has also been applied successfully to aluminum and magnesium. In these metals $[1/N(E_F)][dN(E_F)/d\sigma]$ is, however, not significantly different from the free-electron value in agreement with thermal expansion[54,55] and $dT_c/d\sigma$ data.[56]

VII. SUMMARY

We have measured simultaneously the amplitudes of the torque and the oscillatory magnetostriction of single crystals of gallium at 1.3 K in magnetic fields up to 22 kOe. From these results we have determined the uniaxial stress dependence of various Fermi-surface orbits for stresses parallel to the main crystalline axes. The values for $\partial \ln A/\partial\sigma_i$, where A is the area of the orbit and σ_i is a tension in the positive i direction, are highly anisotropic. For a stress parallel to the c axis, $\partial \ln A/\partial\sigma_i$ is about one order of magnitude smaller than for stresses along the b or a axis. For most of the orbits investigated, $\partial \ln A/d\sigma_a$ and $\partial \ln A/\partial\sigma_b$ are comparable in magnitude, but are of

opposite sign. A similar anisotropy is found for the uniaxial stress dependence of the density of states at the Fermi level. Based on previous work on the Fermi surface of gallium and using our stress dependence data, we suggest a new assignment of extremal orbits obtained by Reed in his calculations of the Fermi surface.

Between 1.4 and 10 K we have measured the linear thermal expansion along the a, b, and c axis; and for the same orientations, we have determined the length changes at the magnetic-field-induced transition from the superconducting to the normal state. From the thermal expansion measurements we have derived the uniaxial stress dependence of the electronic specific heat, and from the length-change experiments we have determined the uniaxial stress dependence of the electron-phonon interaction parameter λ. From these results we have then calculated values for the stress dependence of the band-structure density of states. We find a very pronounced anisotropy in this quantity, namely $\partial \ln N(E_F)/\partial\sigma_a = -7\times10^{-6}$ bar^{-1}, $\partial \ln N(E_F)/\partial\sigma_b = +6\times10^{-6}$ bar^{-1}, and $\partial \ln N(E_F)/\partial\sigma_c = -1.7\times10^{-6}$ bar^{-1}.

Using a very simple parabolic rigid-band model, we calculated $[1/N(E_F)][dN(E_F)/d\sigma]$ from the experimental values of $(1/A)(dA/d\sigma)$. We find qualitative agreement between these values and the $[1/N(E_F)][dN(E_F)/d\sigma]$ derived from thermal expansion and $\partial T_c/\partial\sigma_i$ data.

Note added in proof. Very recently, giant quantum oscillations have been observed in gallium single crystals by N. K. Batra and R. L. Thomas [Phys. Rev. B 8, 5456 (1973)]. From the spin splitting of these oscillations they determined $g = 0.7 \pm 0.1$ for a magnetic field parallel to the b axis (see their Table II). For this they assumed without justification $l = 0$ in their Eq. (3), which means that $\hbar\omega_c > g\mu_B H$. Our values for this g factor show that for these particular orbits the correct choice would be $l = 1$, leading then, using their $m^*/m = 0.0513$ to $g = 39.7$.

ACKNOWLEDGMENTS

We are grateful to Professor J. L. Olsen for his continued interest and encouragement throughout this work. We thank E. Hirt and H. Thomas for helping in growing the single crystals, and for their aid in part of the experiments. We also thank Dr. A. Reinmann of Alusuisse Switzerland for his generous supply of high-purity gallium. Helpful discussions with W. van der Mark and W. Wejgaard are gratefully akcnowledged. This work was in part financially supported by the Schweizerische Nationalfond zur Förderung der wissenschaftlichen Forschung.

*Present address: Dept. of Physics, University of Toronto, Toronto, Ontario 5, Canada.

[1] R. W. Powell, Proc. Roy. Soc. A 209, 525 (1951).

[2] N. V. Zavaritskii, Zh. Eksp. Teor. Fiz. 37, 1506 (1959) [Sov. Phys.-JETP 10, 1069 (1960)].

[3] R. W. Powell, M. J. Woodman, and R. P. Tye, Br. J. Appl. Phys. 14, 432 (1963).

[4] M. Yaqub and J. F. Cochran, Phys. Rev. 137, 1182 (1965).

[5] J. F. Cochran and M. Yaqub, Phys. Rev. 140, 2175 (1965).

[6] R. I. Boughton and M. Yaqub, Phys. Kondens. Mater. 9, 138 (1969).

[7] K. R. Lyall and J. F. Cochran, Can. J. Phys. 49, 1075 (1971).

[8] N. A. Roughton and H. A. Nash, Bull. Am. Phys. Soc. 7, 608 (1962).

[9] (a) J. C. Slater, G. F. Koster, and J. H. Wood, Phys. Rev. 126, 1307 (1962). (b) The a, b, and c given here are the lattice constants of the pseudotetragonal lattice of gallium. The pseudohexagonal unit cell [Ref. 9(a)], has pseudohexagonal symmetry for an axis parallel to the a axis.

[10] V. Heine, J. Phys. C 1, 222 (1968).

[11] A. P. Cracknell, *The Fermi Surface of Metals*, *Monographs on Physics* (Taylor and Francis, London, 1971); Adv. Phys. 18, 681 (1969); 20, 1 (1971).

[12] W. A. Reed, Phys. Rev. 188, 1184 (1969).

[13] A full list of references on these topics is given in Ref. 12.

[14] M. L. Cohen and V. Heine, *Solid State Physics*, edited by H. Ehrenreich, F. Seitz, and D. Turnbull (Academic, New York, 1970), Vol. 24.

[15] I. M. Lifshitz, Zh. Eksp. Teor. Fiz. 38, 1569 (1960) [Sov. Phys.-JETP 11, 1130 (1960)].

[16] B. I. Verkin, L. B. Kuzmicheva, and I. V. Svechkarev, Zh. Eksp. Teor. Fiz. 54, 74 (1968) [Sov. Phys.-JETP 27, 41 (1968)].

[17] B. I. Verkin and I. V. Svechkarev, Zh. Eksp. Teor. Fiz. 47, 404 (1964) [Sov. Phys.-JETP 20, 269 (1965)].

[18] V. I. Makarov and I. Ya. Volynskii, Zh. Eksp. Teor. Fiz. 61, 1928 (1971) [Sov. Phys.-JETP 34, 1026 (1972)].

[19] V. G. Bar'yakhtar, V. V. Gann, V. I. Makarov, and T. A. Ignat'eva, Zh. Eksp. Teor. Fiz. 62, 1118 (1972) [Sov. Phys.-JETP 35, 591 (1972)].

[20] C. W. Chu, T. F. Smith, and W. E. Gardner, Phys. Rev. B 1, 214 (1970).

[21] T. G. Berlincourt and M. C. Steele, Phys. Rev. 95, 1421 (1954).

[22] J. E. Schirber, Phys. Rev. Lett. 28, 1127 (1972).

[23] J. E. Schirber and J. P. Van Dyke, Phys. Rev. Lett. 26, 246 (1971).

[24] J. G. Collins, Ann. Acad. Sci. Fenn. A 6, 239 (1966).

[25] Alusuisse AG, Neuhausen, Switzerland.

[26] D. Shoenberg and P. J. Stiles, Proc. Roy. Soc. A 281, 62 (1964).

[27] P. A. Penz and T. Kushida, Bull. Am. Phys. Soc. 14, 29 (1969).

[28] B. S. Chandrasekhar and E. Fawcett, Adv. Phys. 20, 775 (1971).

[29] R. Griessen and R. S. Sorbello, Phys. Rev. B 6, 2198 (1972).

[30] R. Griessen and R. S. Sorbello, J. Low Temp. Phys.

16, xxx (1974).
[31]G. Brändli and R. Griessen, Cryogenics 13, 299 (1973).
[32]R. Griessen, Cryogenics 13, 375 (1973).
[33]A. Goldstein and S. Foner, Phys. Rev. 146, 442 (1966).
[34]J. Condon, see Ref. 12.
[35]P. Goy, A. Goldstein, D. N. Langenberg, and J. C. Piccard, Phys. Lett. A 25, 324 (1967).
[36]I. M. Lifshitz and A. M. Kosevich, Zh. Eksp. Teor. Fiz. 29, 730 (1955) [Sov. Phys.-JETP 2, 636 (1956)].
[37]J. P. G. Shepherd and W. L. Gordon, Phys. Rev. 169, 541 (1968).
[38]Y. Shapira and B. Lax, Phys. Rev. 138, 1191 (1965).
[39]A. B. Pippard, *Solid State Physics, Electrons in Metals*, edited by J. G. Cochran and R. R. Haering (Gordon and Breach, New York, 1968), p. 19.
[40]A. J. Bennett and L. M. Falicov, Phys. Rev. 136, 998 (1964).
[41]A. Myers and J-R. Bosnell, Philos. Mag. 13, 1273 (1966).
[42]G. F. Koster, Phys. Rev. 127, 2044 (1962).
[43]T. H. K. Barron, Philos. Mag. 46, 720 (1955).
[44]A. B. Migdal, Zh. Eksp. Teor. Fiz. 34, 1438 (1958) [Sov. Phys.-JETP 7, 996 (1958)].
[45]H. R. Ott and E. Hirt (unpublished).
[46]N. E. Philips, Phys. Rev. 134, 385 (1964).
[47]G. Seiden and P. H. Keesom, Phys. Rev. 112, 1083 (1958).
[48]W. L. McMillan, Phys. Rev. 167, 331 (1968).
[49]P. Morel and P. W. Anderson, Phys. Rev. 125, 1263 (1962).
[50]H. R. Ott and R. S. Sorbello, J. Low Temp. Phys. 14, 73 (1974).
[51]H. R. Ott, Solid State Commun. 9, 2225 (1971).
[52]C. Palmy, thesis, No. 4546 (Eidgenössische Technische Hochschule, 1970) (unpublished).
[53]R. Griessen and H. R. Ott, Phys. Rev. Lett. 29, 1159 (1972).
[54]R. D. McCammon and G. K. White, Philos. Mag. 11, 1125 (1965).
[55]J. G. Collins, G. K. White, and C. A. Swenson, J. Low Temp. Phys. 10, 69 (1973).
[56]H. R. Ott, J. Low Temp. Phys. 9, 331 (1972).